J. Chem. Sci. (2020)132:79
https://doi.org/10.1007/s12039-020-01787-0

REGULAR ARTICLE

Synthesis of multilayer polymer-immobilised nanosilver for catalytic study in condensation reaction of aniline and acetylacetone

SUPRIYA, NITAI CHANDRA MAJI, JAYANTA KUMAR BASU and SONALI SENGUPTA*
Department of chemical engineering, Indian Institute of Technology Kharagpur, Kharagpur 721302, India
E-mail: sonalis.iitkgp@gmail.com

MS received 5 December 2019; revised 24 February 2020; accepted 1 March 2020

Abstract. Silver nanoparticles were synthesized in green route with non-hazardous polyvinyl alcohol and polyvinylpyrrolidone as stabilizing as well as reducing agents and water as green solvent. This silver nanoparticle-embedded polymer composite film, Ag/PVA–PVP was characterized by UV–Vis spectroscopy, SEM and TEM. The catalytic activity of this film was evaluated in reduction of p-nitrophenol, acylation of aniline and synthesis of a β-enaminone, 4-phenylamino-pent-3-en-one with appreciably good results. β-enaminone synthesis reaction was chosen to study the effects of kinetic parameters such as reactant quantity, catalyst loading, solvents and temperatures. In a typical reaction, 89% conversion was achieved. A probable chemical reaction mechanism is suggested. Kinetic model fitting for the synthesis of β-enaminone reaction was done for the first time here. Heterogeneous kinetic model following Eley-Rideal pathway showed an excellent data fitting for the reaction. The rate law parameters were estimated.

Keywords. β-Enaminone; heterogeneous catalyst; microwave irradiation; silver nanoparticles; green synthesis.

1. Introduction

Silver nanoparticles (Agnp), owing to their unique chemical and physical properties exhibit wide spread applications in versatile fields.[1–5] Agnp shows exceptional catalytic efficacy in numerous organic reactions.[6–11] The Agnp-based catalyst is somewhat more favored over other metal nanoparticles, for instance, palladium, gold, and platinum, because of the ease of preparation and lower cost.

Enhanced catalytic activity of metal nanoparticles is the consequence of their high surface to volume ratio, although the difficulty in retrieving the nanoparticles from product stream creates a considerable disadvantage of their repeated use. Hence, the catalytic nanoparticles should be provided support grid which helps in separation and recycle. Well-proven catalytic performances of polymer composites on noble metals like Rh, Pt, Pd was observed in nitro aromatics, hydrogenation of cyclohexene, hydrosilylation of alkenes, unsaturated aldehydes and alcohols.[12–18] Among many other conventional carriers such as TiO_2, C, SiO_2, Al_2O_3, and zeolites, polymeric supports offer versatile features as potential carriers. Polymers have high capability to stabilize uniformly dispersed metal nanoparticles, hydrophilic/hydrophobic character and the presence of several functional groups and hence, all these make them very attractive supporting materials.[19,20] As a result, catalytic centers formed in polymer matrix fundamentally differ from that of conventional inorganic carrier-supported noble metal catalysts.[20]

β-enaminones are esters which are profoundly used as synthons in the synthesis of various natural products, heterocyclic compounds, and bio-active heterocycles such as pyridinones, therapeutic agents with antibacterial, antitumor, anticonvulsant, and anti-inflammatory properties.[21–26] Considering their immense importance, it is necessary to have a convenient and effective process for β-enaminones synthesis. Among the various methods developed for the synthesis of β-enaminones, condensation of dicarbonyl compound with amines in aromatic solvent followed by azeotropic removal of water was the most straightforward and simple method. Non-conventional methods include ultrasound and

*For correspondence

Electronic supplementary material: The online version of this article (https://doi.org/10.1007/s12039-020-01787-0) contains supplementary material, which is available to authorized users.

Published online: 26 June 2020

microwave techniques for synthesis of β-enaminones.[27,28] Some other methods were found which applied various catalysts such as $Yb(OTf)_3$, perchlorates, $Zn(OCl)_4$, $InBr_3$, and $CoCl_2$, etc.[29–34] Although these methods are claimed as modified ones yet they suffer several drawbacks which include the use of homogeneous, expensive and non-reusable catalyst, use of hazardous organic solvent and high temperature reaction. Therefore, it is important to develop a heterogeneous, recyclable, and non-toxic catalyst for synthesis of β-enaminones at mild operating condition.

Polymer-supported Agnp are evaluated in the reduction of *p*-nitrophenol or dyes reduction in most of the studies.[35] Polymer supported palladium nanoparticles are found in applications such as Suzuki-Miyaura, cross-coupling reaction and Sonogashira reaction, Mizoroki-Heck reaction, reduction of *p*-nitrophenol and organic dyes.[36–39] Agnp is an established catalyst in oxidation and reduction of a number of molecules. Recently, colloidal silver is used in C-C coupling reaction.[40] In the current study, PVA–PVP mixed polymer matrix is chosen as the support for Agnp. PVA has excellent film forming, emulsifying and adhesive properties, and PVP helps in reduction of size of nanoparticles[41] PVA–PVP mixed matrix as a support for Agnp is not only cheap and eco-friendly but this also serves as reducing and stabilizing agents. In spite of these advantages, the major inconvenience associated with this composite catalyst is the reaction of PVA–PVP film with the oxidizing agents when used in oxidation environment and as a result, the film gets dissolved in the reaction medium. In the present work, PVA–PVP supported Agnp film was successfully used as catalyst in several other important reactions such as reduction, condensation and acylation reaction. The composite polymer film PVA–PVP was prepared where Agnp are embedded, and the film was used as a catalyst for the synthesis of 4-phenylamino-pent-3en-one (a β-enaminone) by the reaction of acetylacetone and aniline at mild condition. Moreover, the performance of the catalyst was also tested in *p*-nitrophenol reduction reaction at room temperature and acylation reaction of aniline with acetic acid at 373 K as well. The heterogeneous kinetic model for β-enaminone synthesis reaction has been proposed and rate law parameters are estimated.

2. Experiment

2.1 *Materials*

Polyvinyl alcohol (1,46,000–1,86,000 m.w., + 99% hydrolysis) and polystyrene (280,000 m.w) were purchased from M/s. Sigma-Aldrich, India. Polyvinylpryrrolidone (30 K) and *p*-nitrophenol (98%) were obtained from M/s. Loba Chemie, India. Silver nitrate (≥99%), toluene (≥99%), sodium borohydride (≥95%), acetylacetone (99%), aniline (≥99%) and acetic acid (glacial) (≥99.98) were procured from M/s. Merck India Ltd., India. HPLC grade methanol (99.8) was purchased from Rankem, India. All the experiments were performed using double distilled water.

2.2 *Characterization*

SHIMADZU UV 1800, Japan UV–VIS spectrophotometer of range 200–1100 nm was used to obtain electronic spectra. Transmission electron microscopy (TEM) was conducted on TECNAI G2 20S TWIN, FEI, USA TEM at an accelerating voltage of 120 kV. A thin film was placed on copper grid and vacuum dried. Field emission scanning electron microscopy (FESEM) was performed on JSM-7610F, JEOL Japan. Silver concentration in the film was evaluated by atomic absorbance spectroscopy (AAS) using iCE3300 AA Spectro, Thermo Fisher (USA). Gas chromatography (Perkin Elmer Clarus 480 with DB5, capillary column) was used to monitor the progress of all the reactions by reaction sample analysis and the conversion was estimated. Products were confirmed by Gas Chromatogram-Mass Spectroscopy (GC-MS) with Agilent 7890A GC and 240 ion trap MS using DB-5 column.

2.3 *Synthesis of PVA/PVP/Agnp film*

Scheme 1 shows the schematic diagram of synthesis process of Agnp supported multilayered composite film. A solution of polystyrene (PS, 1 g) in toluene (7 ml) was used for making PS layer on glass substrate to use that as a sacrificial layer. Three sets of PVA 6% (w/v) solution at 353 K and similarly three sets of PVP 6% (w/v) at room temperature were prepared with deionized water. These solutions were then mixed at 358 K under stirring for an hour to prepare three solutions with PVA:PVP ratios of 95:5, 90:10 and 85:15 (wt/wt). $AgNO_3$ solution was prepared and mixed in these solutions to get Ag: polymer blend (PVA–PVP solution is designated as polymer blend, PB) ratio of 0.16 (wt/wt). One more mixture was prepared with PVA and $AgNO_3$ in deionized water with the same ratio of 0.16 (wt/wt) of Ag:PVA to prepare composite of Ag/PVA.

A basic requirement for the catalytic film is that it should be thin enough for reactants to get an easy access to the nanoparticles spread on that, but thick enough to prevent rupture. A three-layered film with the top and bottom layers made with Ag-PB and with the middle layer made up of PVA can provide the sufficient thickness. While preparing this sandwich-type film, a polystyrene (PS) layer is also required which will act as a sacrificial layer and will not come as a component of the actual composite catalyst film. Thus, the initial film is a PS/(Ag-PB)/PVA/(Ag-PB) film which is prepared on a glass substrate/slide with PS layer stuck on the slide.

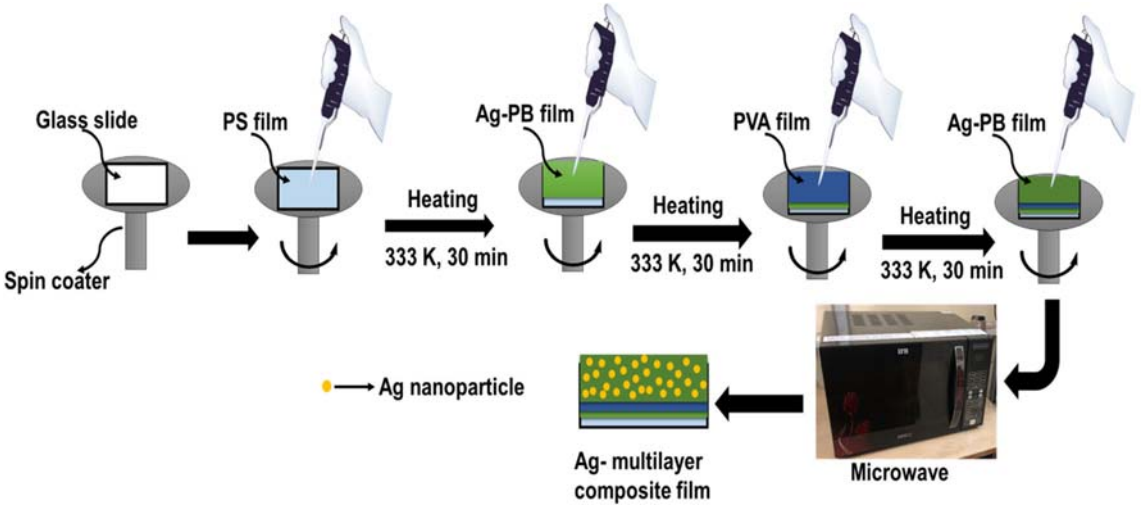

Scheme 1. Schematic diagram of synthesis process of Ag-nanoparticles supported multilayered composite film.

To prepare this film, these solutions were spin coated on a glass slide to form polymer layer one after another with such a fashion that a layer of PVA is sandwiched between two Ag-PB or Ag-PVA layers. The stepwise preparation process of this complex composite is stated below.

Solution of PS was coated on glass substrate at 1000 rpm for 20 s with the help of spin coater. The coated film was heated at 333 K for 30 min.

Ag-PVA or Ag-PB solution was spin-coated on this PS layer at 500 rpm for 10 s followed by 6000 rpm for 10 s and this composite film was heated at 333 K for 30 min.

In the third step, pure PVA solution (5% wt/v) was spin-coated at 500 RPM for 10 s followed by 4000 rpm for 10 s on the previous composite film and then heated at 333 K for 30 min.

In the final step, Ag/PVA or Ag/PB solution was again spin-coated as the second layer at 500 rpm for 10 s followed by 6000 rpm for 10 s to make PS/(Ag-PVA or Ag-PB)/PVA/(Ag-PB or Ag-PVA) film. Now, they altogether were treated under microwave irradiation for different times to get the Agnp supported composite film of different characteristics.

The film prepared, however, is not yet suitable for reaction, since it is still attached to the glass substrate. This is where the need of PS sacrificial layer comes to play. The glass substrate with polymer composite film on it is immersed into toluene, which dissolves the sacrificial layer, thereby, removing the catalytic film from the glass slide easily and without rapture. The composite films thus prepared are kept separately on Teflon plate to avoid sticking up with one another.

3. Test of catalytic activity in different reactions

3.1 *Para-nitrophenol reduction reaction*

The activity of composite polymer-Agnp catalyst was evaluated primarily in *p*-nitrophenol (*p*-NP) reduction reaction. Freshly prepared 10 ml of aqueous sodium borohydride (0.1 M) was mixed with 0.1 ml of aqueous *p*-NP (0.1 M) taken in a vial and connected with magnetic stirrer. The polymer film (contain 6.2 μg of Agnp), amount of silver in the film was determined by AAS analysis) wrapped Teflon frame was put in the reaction mixture at ambient temperature for 24 min and 100% conversion of p-NP was observed. Progress of the reaction was monitored by UV–Vis spectrometry in the scanning range of 250–500 nm.

3.2 *Acylation reaction of aniline*

To verify the catalyst performance, aniline acylation reaction was chosen. 12 mmol aniline was mixed with 12 ml acetic acid (0.21 mol) in a vial connected with magnetic stirrer. Four (Ag-PB)/PVA/(Ag-PB or Ag-PVA) composite films (22.8 μg of Agnp, as determined from AAS analysis) encased in Teflon frame were placed in sample vial. It was then heated in oil bath at 373 K. The progress of the reaction was monitored by GC analysis, and 94% conversion of aniline was achieved in 4 h.

3.3 *Synthesis of β-enaminone*

Typical reaction for synthesis of a β-enaminone, 4-phenylamino-pent-3-en-one from acetylacetone and aniline has been carried out by mixing 1 mmol aniline and 1 mmol of acetylacetone in 12 ml methanol in a vial connected with magnetic stirrer (Scheme 2). Four (Ag-PVA or Ag-PB)/PVA/(Ag-PB or Ag-PVA) composite films (22.8 μg of Agnp as obtained from AAS analysis) Agnp were encased in Teflon frame and

placed in sample vial. The vial was then heated in oil bath at 333 K. The progress of the reaction was monitored by GC analysis and product was confirmed by GC-MS analysis. This reaction has been performed with parameters study and their estimation.

4. Results and Discussion

In the synthesis of (Ag-PVA or Ag-PB)/PVA/(Ag-PB or Ag-PVA) composite film, hydroxyl group of PVA reduces Ag^+ to Ag. Microwave irradiation helps to accelerate reduction of Ag^+ to Ag. Silver nanoparticles show optical spectrum in terms of absorption peak, also known as the surface plasmon resonance (SPR). Figure 1 shows the UV–Vis absorption spectrum for films prepared from PVA:PVP (95:5) solutions and kept for 8 min under microwave irradiation. A sharp peak was observed at 423 nm which confirms the formation of mono-dispersed Agnp in the film.

The morphology of Agnp supported PVA films, prepared at different time periods of microwave irradiation times is shown as SEM image in Figure 2a–c. All the SEM images confirm that irradiation time has significant effect on the size and dispersity of Agnp in the film. Agnp formed after 6 min irradiation time are found to be larger in size (20 nm, Figure 2a), compared to that formed after 8 min irradiation (11 nm, Figure 2b). Moreover, increase in irradiation time changes the polydispersed pattern of Agnp into monodispersed form in the polymer film as shown in inset of each image of Figure 2. The reason behind this phenomenon may be extent of chemical reduction as well as digestive ripening (it is process in which larger Ag particles converted into smaller ones).[42–44] The large particles (20 nm) obtained at 6 min may be the agglomerated form of Agnp. The difference in sizes of the Agnp formed, i.e. 11 nm and 12 nm (Figure 2b, c) from the synthesis time of 8 min and 10 min respectively is insignificant. Hence, 8 min irradiation time is considered to be the most preferred one for synthesis of small sized nanoparticles with good dispersion. The variation of particle size of Agnp prepared at different microwave irradiation times and different PVA/PVP ratios is tabulated in Table 1. The overall thickness of multilayer composite film was found to be 25–26 μm, measured using a digital micrometer.

The morphology of Agnp embedded polymer films with different concentrations of PVA–PVP is depicted in Figure 3a–d. The PVP content in PVA is increased from 0 to 15% and the compositions of polymer mixture taken are 100% PVA (Figure 3a), (95:05), (90:10) and (85:15) % PVA:PVP (Figure 3b–d) by weight. Agnp are produced in all these polymers using the same concentration of $AgNO_3$ as Ag precursor. The homogeneously distributed small spherical particles represent Agnp in all micrographs. The insets in all the pictures show the particle size distribution for each case and it is clearly visible that, with increase in PVP from 0 to 15%, the average size of Agnp shifts from 11 nm to 6.5 nm. This indicates that PVP prevents agglomeration of nanoparticles and reduces the size of them. The PVP polymer contains both hydrophilic (pyrrolidone moiety) as well as hydrophobic (alkyl moiety) components. This effect of PVP may be explained by the strong affinity of N and O atoms of its polar group (pyrrolidone group) towards Ag^+ ions which stabilizes it. On the other hand, the hydrophobic methylene and methyne groups in the ring along with the backbone of PVP molecule prevent the

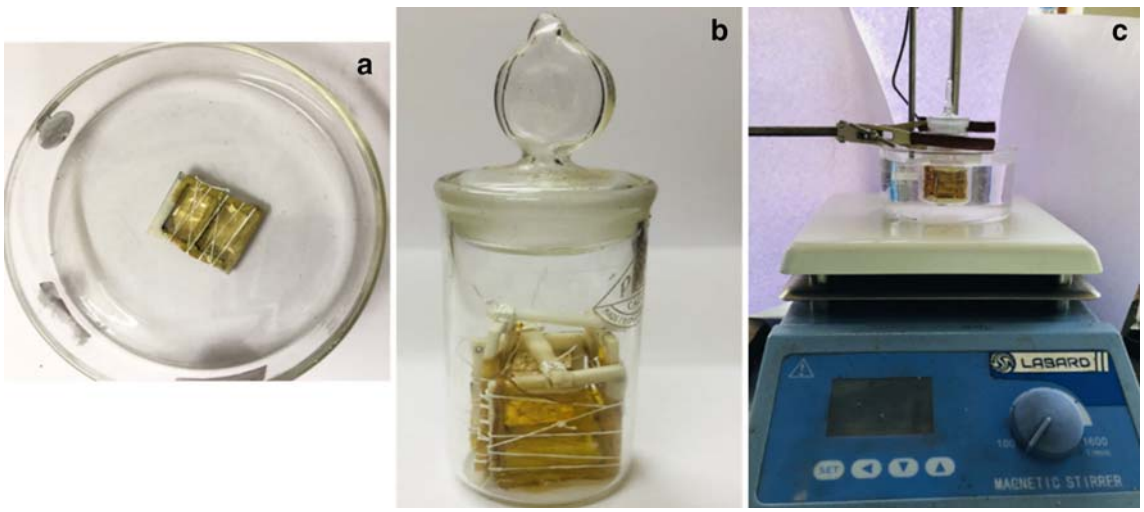

Scheme 2. Images of (a) film wrapped in teflon frame, (b) reaction vial with catalyst films, (c) overall experimental setup.

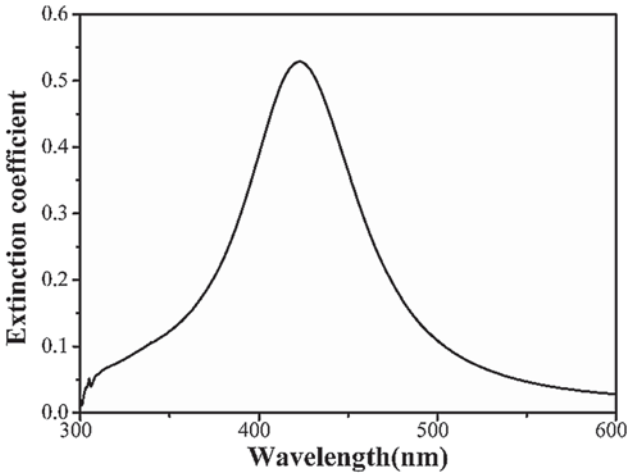

Figure 1. UV–Vis spectra of Agnp supported PVA–PVP (95:5) film at 8 min microwave irradiation time.

agglomeration of Agnp by repulsive force.[41,45,46] Because of the presence of PVP, the rate of spontaneous nucleation increases, as a result, the number of final nanoparticles increases, and therefore the mean particle size decreases. More PVP acts as a favorable factor and the size of Agnps decreases. At the same time, the resultant metallic silver particles are capped faster by PVP molecules of higher concentration than by that of the lower.

TEM image of Agnp supported PVA/PVP film of PVA:PVP (90:10) obtained with 8 min microwave irradiation time is shown in Figure 4. The image confirms the formation of mono dispersed and non-aggregated Agnp. Average size of the particles estimated from histogram of TEM image (inset of Figure 4) was found to be 6±1.6 nm. TEM image shows somewhat smaller size of the Agnp than that observed from SEM analysis. The difference in size may be due to the use of a single thin film for TEM analysis compared to three-layered film used for SEM.

4.1 *Catalyst test: Reduction of p-nitrophenol*

Activity of the prepared composite catalyst was first verified in the reduction of *p*-NP to *p*-aminophenol

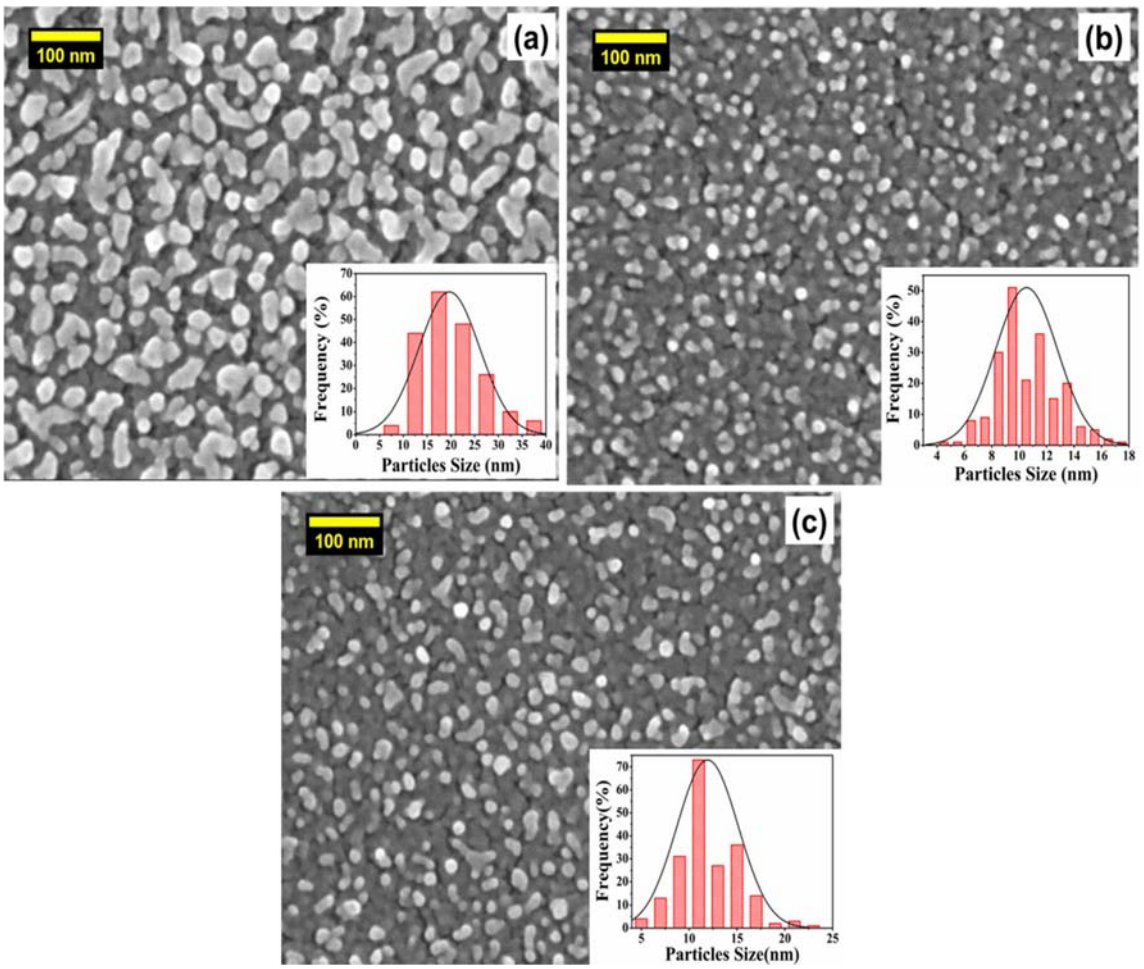

Figure 2. SEM images of Agnp supported PVA film at different microwave irradiation times (a) 6 min (b) 8 min (c) 10 min.

Table 1. Particle size of Agnp at variable microwave irradiation times and different PVA/PVP ratios at constant irradiation time of 8 min as obtained from SEM analysis.

Parameter		Average Agnp size (nm)
Micro wave irradiation time (min) (Agnp/PVA)	6	20 ± 6
	8	11 ± 2
	1 0	12 ± 3
PVA:PVP (8 min irradiation time)	100:0	11 ± 2
	95:05	10 ± 2
	90:10	9 ± 2
	85:15	6.5 ± 2

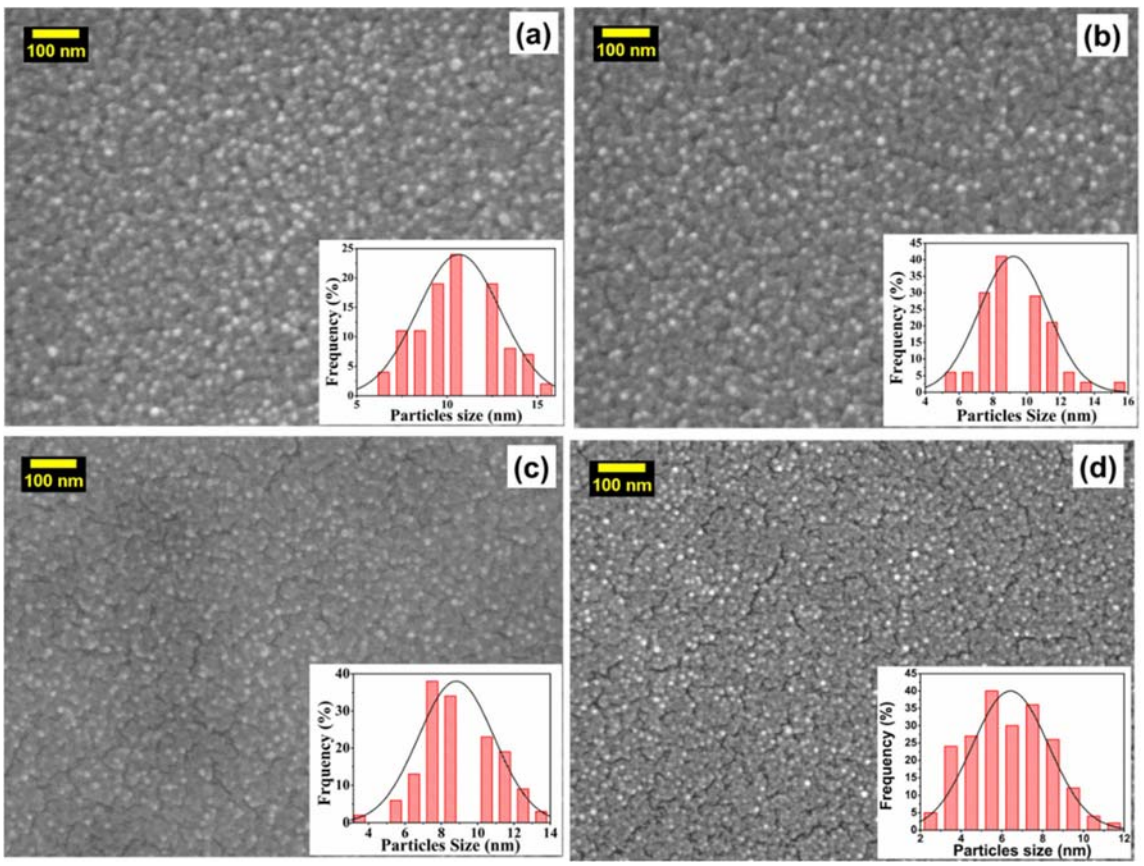

Figure 3. SEM image of silver nanoparticles supported PVA/PVP film at different PVA:PVP ratios (a) 100:0 (b) 95:05 (c) 90:10 (d) 85:15.

(*p*-AP) with excess of sodium borohydride. This reaction is used as a model reaction for catalyst activity test. *p*-AP is an important raw material for synthesis of medicine, lubricant and dyes. *p*-NP is a hazardous pollutant present in industrial wastewater which is unwanted for safe water use. Hence, it is necessary that the catalyst for the reaction should be such that it can convert *p*-NP completely at economic process condition. Figure 5 shows the absorbance of *p*-NP at 400 nm wavelength which decreases with time and simultaneously the absorbance of *p*-AP at 300 nm wavelength increases with time. Absorption peak of *p*-NP was completely disappeared in 24 min and this confirms total conversion of *p*-NP into *p*-AP. Plot of $\ln(A_t/A_o)$ with time (inset of Figure 5) shows a linear fitting according to equation (1) with good correlation coefficient ($R^2 = 0.99$), which confirms first order rate kinetics of the reaction. Apparent rate constant (k_{app} from equation 1) estimated from the slope of this linear plot is found to be 0.16 min^{-1}. Reaction was

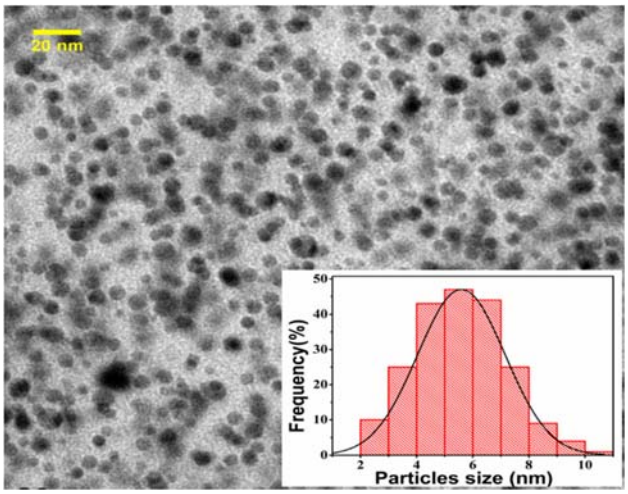

Figure 4. TEM image of silver nanoparticles supported PVA/PVP film at PVA:PVP (90:10) obtained at 8 min microwave irradiation time.

repeated for five consecutive times with the same catalyst film by washing with water and drying. After each run the activity of the catalyst is found to remain same from fresh to 5th time reuse.

$$\frac{dC_{NP}}{dt} = k_{app}C_{NP}$$

$$ln\frac{A_t}{A_0} = ln\frac{C_t}{C_0} = k_{app} \times t \quad (1)$$

Where C_{NP} is concentration of *p*-NP, k_{app} is apparent rate constant, C_t and C_o represent concentrations of *p*-NP at different time and initial absorbance respectively, A_t and A_o represent absorbance at different time and initial absorbance respectively. Turnover frequency (TOF) and turnover number (TON) of catalyst are two significant parameters to compare catalyst efficacy. TON can be defined as number of moles of reactant consumed per moles of catalyst and TOF is simply calculated by dividing TON/Time of reaction. TOF and TON was found to be 0.121 s^{-1} and 174 respectively, which is higher when compared with litreature as shown in Table S1 in supplementary file.

4.2 *Catalyst test: acylation reaction*

Another verification of catalytic activity of the composite film was done in acylation reaction of aniline with acetic acid at 373 K and 94% conversion of aniline was observed after 4 h. Reusability of catalyst film was tested for two consecutive times with 90% and 84% conversion, which proves that the catalyst film can be successfully used for acylation reaction.

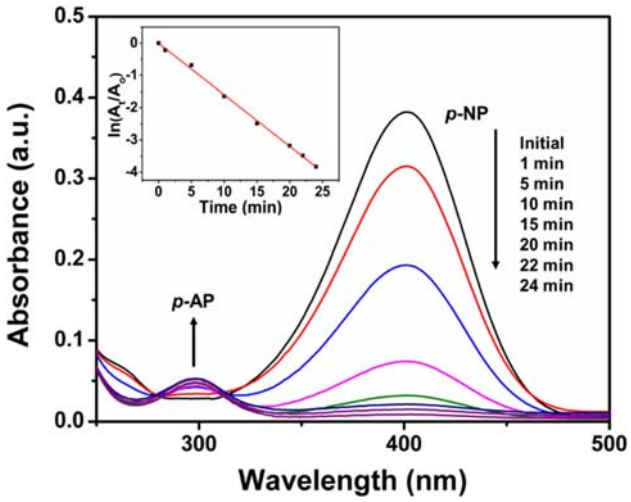

Figure 5. UV-spectra of reduction of *p*-NP to *p*-AP, inset: plot of $ln(A_t/A_o)$ with time.

4.3 *Catalyst test: synthesis of β-enaminone*

The third reaction to which the performance of catalyst has been tested is the synthesis of β-enaminone, 4-phenylamino-pent-3en-one, formed by the reaction of acetylacetone and aniline. The effect of different kinetic parameters on the reaction has been estimated. The results of the detailed study are stated and a heterogeneous kinetic model for this reaction is also proposed.

4.3a *Effect of acetylacetone and aniline amount*: Effect of acetylacetone on conversion of aniline is shown in run 1–7 of Table 2. As the amount of acetylacetone increases from 0 to 2 mmol, conversion of aniline increases from 0 to 96% for 12 h run, keeping aniline at 1 mmol. Gradual increase in acetylacetone to 3, 4, and 5 mmol, keeping the aniline (1 mmol) amount constant, 96% conversion was estimated at much reduced time of 8, 4, and 2 h respectively. Similarly, the effect of aniline on conversion is shown in run 9–11 of the table. As the amount of aniline increases from 0.5 to 1 mmol, keeping the amount of acetylacetone fixed at 1 mmol, the conversion of aniline decreases from 93.62 to 67.76%. This indicates that with increase in quantity of acetylacetone, conversion of aniline increases or reaction rate is enhanced, whereas, with increase in amount of aniline the conversion decreases or reaction rate reduces. Run 8 reveals the result of the reaction of 1 mmol acetylacetone with 1 mmol aniline with 89% conversion in 19 h. The chemical reaction mechanism and stoichiometric reaction equation are discussed in section 4.3g and shown in Figure 8.

4.3b *Effect of catalyst loading*: Figure 6 shows the effect of amount of catalyst on conversion of aniline. The results show that as the amount of catalyst increases from 0 to 22.8 μg, conversion increases from 5 to 69% in the reaction time of 12 h. This result is a clear consequence of the increase in

active site with the increase in the amount of the catalyst. More number of active sites result higher adsorption of acetylacetone on the sites which reflects increase in conversion.

4.3c *Effect of temperature*: The reaction was carried out in the temperature range from 303 to 333 K for 12 h and aniline conversion is found to increase from 0 to 68% with increase in temperature, which is shown in Figure 7. This trend follows Arrhenius equation, which says that the rate of reaction increases with temperature and that reflects an increase in conversion.[47] Hence, the temperature has a pronounced effect on the reaction and the conversion follows the usual trend with temperature.

4.3d *Effect of size of silver nanoparticles*: PVA and PVP ratio shows considerable effect on the reaction, as PVP % increases from 0 to 15%, size of the silver nanoparticles decreases from 11 nm to 6.5 nm and conversion of aniline increases from 47 to 70%. Smaller size nanoparticles import better conversion than the larger ones. As discussed earlier, PVP concentration has a noticeable effect on the size of Agnp and size decreases with the introduction of PVP to PVA. This decrease in Agnp size is also associated with the increase in conversion of aniline. At 100% PVA with no PVP, the average particle size is observed to be 11 nm and the conversion is 47%, whereas, with 95:5 and 90:10 of PVA:PVP mixture, the particles size become 10 nm and 9 nm with corresponding conversion 51% and 68% respectively. Decrease in particle size of Agnp provides higher conversion, which may be the result of the availability of more number of Agnp and hence catalytic centers too.[48] Further increase in PVP percentage in 85:15 PVA:PVP mixture, particle size decreases to 6.5 nm with insignificant increase in conversion to 70%. This indicates that further decrease in size does not help in increasing conversion. Hence, it can be inferred that, smaller Agnp is responsible for higher conversion, which is a reflection of the effect of PVP content in the support as well. Although continuous addition of PVP to the polymer mixture does not produce any gain to the conversion yet the chance of the polymer film to become soluble in the reaction medium increases.

4.3e *Effect of solvent*: To investigate the effect of solvent on the conversion, the reaction was carried out with two different solvents, methanol and toluene for 12 h, keeping the amount of the reactant constant for each case. The reaction in methanol as solvent resulted 68% conversion of aniline at 333 K, while the same conversion was achieved at higher temperature, 363 K with toluene as solvent. This

Table 2. Conversion of aniline with different amounts of acetylacetone[§].

Run no.	Aniline (mmol)	Acetylacetone (mmol)	Conversion of aniline (%)	Time (h)
1	1	0	0	12
2	1	1	67.79	12
3	1	1.5	71.72	12
4	1	2	96.21	12
5	1	3	96.12	8
6	1	4	96	4
7	1	5	96.56	2
8	1	1	89	19
9	0.5	1	93.63	12
10	0.75	1	82.45	12
11	1	1	67.76	12

[§]Reaction condition: catalyst (PVA:PVP= 90:10, 22.8 μg of Agnp), 333 K, methanol (12 ml).

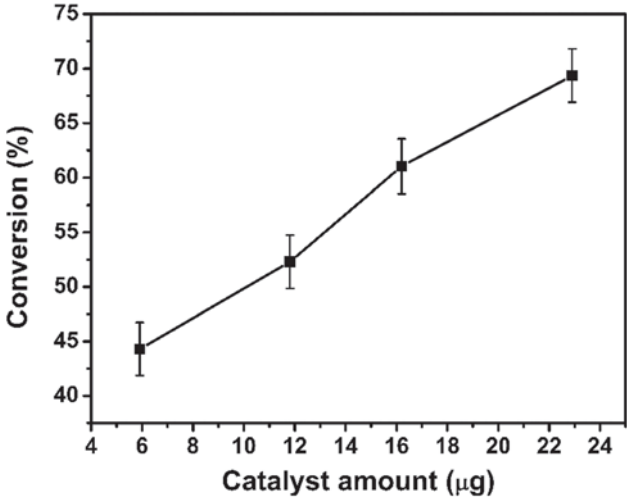

Figure 6. Effect of catalyst amount on conversion of aniline. Reaction condition: acetylacetone (1 mmol), aniline (1 mmol), catalyst (PVA:PVP= 90:10), 333 K, methanol (12 ml) and time (12 h).

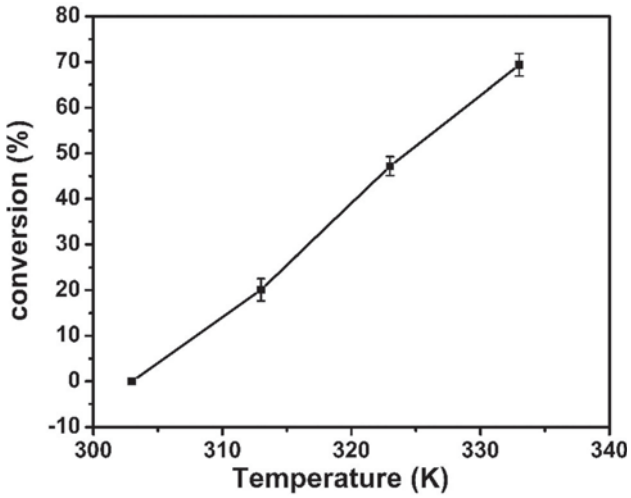

Figure 7. Effect of temperature on conversion of aniline. Reaction condition: acetylacetone (1 mmol), aniline (1 mmol), catalyst (PVA:PVP= 90:10, 22.8 μg of Agnps), methanol (12 ml) and time (12 h).

Table 3. Values of E-R model fitting (polymath 6.0 software).

Variables	Value	95% confidence	R^2	Adj. R^2
k	0.003	8.96E−08	0.99	0.98
K_A (l/mol)	0.020	3.31E−06		
K_P (l/mol)	0.213	7.16E−06		

Table 4. Reusability of catalyst.

Number of runs	1st	2nd	3rd	4th
Conversion %	89	70	65	65

Reaction condition: acetylacetone (1 mmol), aniline (1 mmol), catalyst (PVA:PVP= 90:10, 22.8 μg of Agnp), methanol (12 ml) and time (19 h).

effect can be explained by comparing the polarity of the two solvents. Methanol is a polar solvent whereas toluene is non-polar. The composite polymer catalyst is hydrophilic and hence it gets a friendly environment in methanol than toluene. Moreover, strong hydrogen bond interaction in methanol stabilizes the reaction intermediates and enhances the rate of reaction.[49,50]

4.3f *Heterogeneous kinetic studies*: The effect of variation in concentration of acetylacetone in the reaction shows that as the concentration of acetylacetone increases, more and more atoms are adsorbed on the surface of the catalyst and easily converted into β-enaminone by the reaction with aniline. On the other hand, increase in concentration of aniline hinders the adsorption of acetylacetone molecules and lowers the conversion. Hence, it can easily be concluded that aniline remains in the bulk phase and does not adsorb on the catalyst site. This study helps to select Eley-Rideal model with surface reaction as rate controlling step, the best suitable one for the reaction. Moreover, perfect fitting of the experimental data with adjusted $R^2 = 0.99$ (Table 3) proves the proper selection of the model. Moreover, the 95% confidence values as shown in the table are small enough to confirm the good fitting of the model with experimental data. Overall rate of reaction has been calculated by using equation 2. The heterogeneous kinetic mechanism involves three steps (a) adsorption of acetylacetone (equation 3), (b) surface reaction (equation 4) and (c) desorption of product (equation 5). The Eley-Rideal mechanism was represented in equation 6.

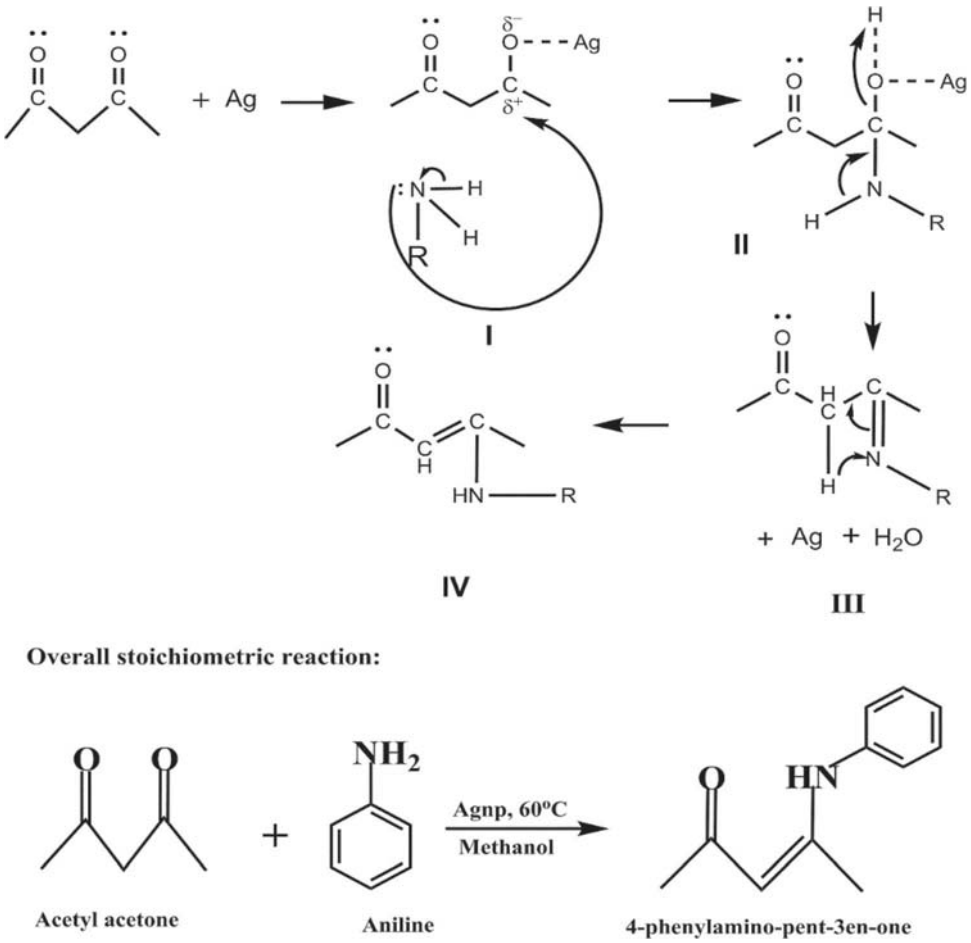

Figure 8. Proposed mechanism for synthesis of β-enaminone (4-phenylamino-pent-3en-one).

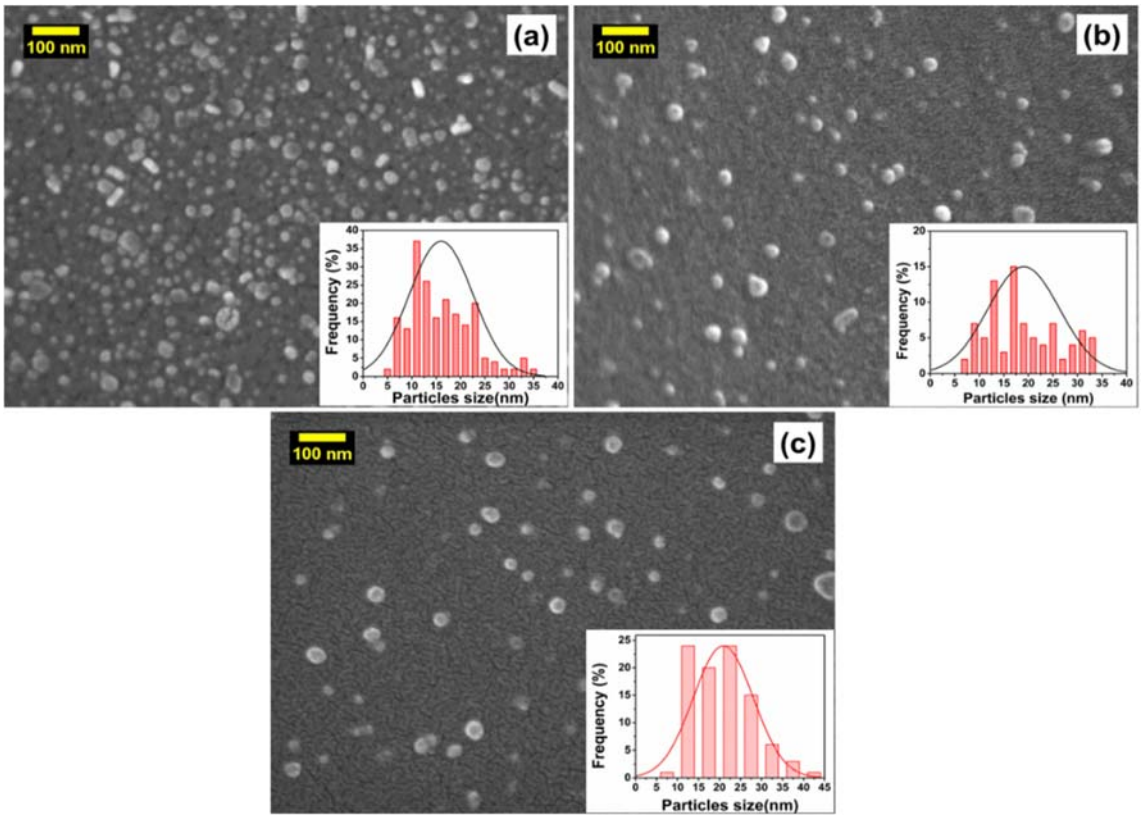

Figure 9. SEM image of catalyst film after (a) 1st run, (b) 3rd run, (c) 4th run.

Overall rate of reaction can be stated as,

$$-r_A = \frac{1}{W}\frac{dC_A}{dt} \tag{2}$$

Where, r_A= rate of the reaction (mol/g.min), W= weight of the catalyst (mg/l), C_A = concentration of acetylacetone (mM), t = time (min).

Now, considering heterogeneous kinetic model, according to the Eley-Rideal irreversible surface reaction controlling mechanism where aniline is not adsorbed on the catalyst, the steps involved are,

$$\mathrm{A} + \mathrm{S} \leftrightarrow \mathrm{A.S} \quad (\text{Adsorption of A}) \tag{3}$$

$$\mathrm{A.S} + \mathrm{B} \rightarrow \mathrm{P.S} \quad (\text{Surface reaction}) \tag{4}$$

$$\mathrm{P.S} \leftrightarrow \mathrm{P} + \mathrm{S} \quad (\text{Desorption of P}) \tag{5}$$

Where, A and B are acetylacetone and aniline respectively, S is the vacant active site of the catalyst and P is the product. A.S and P.S are the adsorbed species on the active sites.

The expression of rate according to this model is stated as,

$$r = \frac{kC_AC_B}{(1 + K_AC_A + K_PC_P)} \tag{6}$$

Where, C_A, C_B and C_P are concentrations of acetylacetone, aniline and product (4-phenylamino-pent-3en-one) respectively. k constant obtained from combined rate parameters. K_A and K_P are adsorption equilibrium constants of acetylacetone and product respectively.

4.3g *Proposed mechanism for synthesis of β-enaminone*: Owing to a single electron in the outermost orbital of Ag [(Kr) $4d^{10}5s^1$], it attracts the electron cloud of one of the carbonyl oxygen atoms of acetylacetone and forms a labile band.[47] Carbon in that carbonyl group, becoming an electrophilic center, attracts one of the lone pairs from nitrogen of aniline molecule and produces an intermediate (II). This after molecular arrangement in step (III) removes water and makes the catalyst Ag free with the formation of the product β-enaminone, 4-phenylamino-pent-3en-one (IV). The mechanism shows a stoichiometry of 1:1 of aniline to acetylacetone. This proposed mechanism is depicted in Figure 8.

4.3h Reusability of the catalyst film: A study of reusability of catalyst for a reaction is an essential part to fulfill the thorough investigation. After each set of run catalyst film was washed with ethanol and vacuum dried for further use. Hence, the catalyst was reused up to 4th run and gradual decrease in conversion is observed, from 89% with fresh catalyst to 65% at 4th run (Table 4). To inquire about

the particles size of Agnp, SEM was done after the 1st run, 3rd and 4th run it has been found that the Agnp size was increased from 9 to 16±6 nm after 1st run (Figure 9a) and increase to 19±6 nm and 20±7 nm after 3rd and 4th run (Figure 9(b, c)) respectively. The decrease in conversion may be a result of increase in size of Agnp. The difference in particles sizes between the Agnp obtained after 3rd and 4th runs is not appreciable and the conversion obtained is also the same as observed from the table. TON and TOF of catalyst is calculated for β-enaminone reaction are found to be 4731 and 249 h^{-1} or 0.069 s^{-1} respectively.

5. Conclusions

An environment friendly protocol has been used for synthesis of silver nanoparticles embedded polymer composite film. Nontoxic and naturally benign PVA and PVP were used as reducing agents, stabilizing agents and supports for nanoparticles. Use of microwave irradiation is a part of this green synthesis method. SEM, TEM and UV–Vis spectrometry analysis confirm the formation of silver nanoparticles in the polymer composite film. Amount of silver nanoparticles in the film was determined by AAS analysis. This work shows the catalytic activity of the nano silver/polymer film in reduction of *p*-nitrophenol, acylation reaction of aniline and β-enaminone (4-phenylamino-pent-3en-one) synthesis. The heterogeneous kinetic model for β-enaminone synthesis reaction has been proposed and rate law parameters are estimated. This study shows that the reaction mechanism follows Eley-Rideal kinetic model with excellent experimental data fitting.

Supplementary Information (SI)

Supplementary information encloses GC-MS spectra of the product, β-enaminone (4-phenylamino-pent-3en-one) (Figure S1 & S2). Comparison of catalyst efficacy with literature-reported catalysts in p-nitrophenol reduction reaction is shown in Table S1. Supplementary information is available at www.ias.ac.in/chemsci.

Acknowledgements

Authors gratefully acknowledge the technical support obtained from Prof. J. Chakraborty, Particle Technology Laboratory, Chemical Engineering Department, Indian Institute of Technology Kharagpur, India.

Funding

This research was carried out solely under the usual funding received from IIT, Kharagpur, India, without any specific grant from funding agencies in the public, commercial, or non-for-profit sectors.

References

1. Rai M, Yadav A and Gade A 2009 Silver nanoparticles as a new generation of antimicrobials *Biotechnol. Adv.* **27** 76–83
2. Zhang H W, Liu Y and Sun S H 2010 Synthesis and assembly of magnetic nanoparticles for information and energy storage applications *Front. Phys. China* **5** 347–356
3. Li Y, Wu Y and Ong B S 2005 Facile synthesis of silver nanoparticles useful for fabrication of high-conductivity elements for printed electronics *J. Am. Chem. Soc.* **127** 3266–3267
4. Li Q, Mahendra S, Lyon D Y, Brunet L, Liga M V, Li D and Alvarez P J J 2008 Antimicrobial nanomaterials for water disinfection and microbial control: potential applications and implications. *Water Res.* **42** 4591–4602
5. Cobley C M, Skrabalak S E, Campbell D J and Xia Y 2009 Shape-controlled synthesis of silver nanoparticles for plasmonic and sensing applications *Plasmonics* **4** 171–179
6. Xu R, Wang D, Zhang J and Li Y 2006 Shape-dependent catalytic activity of silver nanoparticles for the oxidation of styrene *Chem. Asian J.* **1** 888–893
7. Mitsudome T, Arita S, Mori H, Mizugaki T, Jitsukawa K and Kaneda K 2008 Supported silver-nanoparticle-catalyzed highly efficient aqueous oxidation of phenylsilanes to silanols *Angew. Chemie - Int. Ed.* **47** 7938–7940
8. Cong H, Becker C F, Elliott S J, Grinstaff M W, Porco J A, Discovery T and Diels A 2010 Silver nanoparticle-catalyzed Diels -Alder cycloadditions of 2′-hydroxychalcones *J. Am. Chem. Soc.* **132** 7514–7518
9. Baruah B, Gabriel G J, Akbashev M J and Booher M E 2013 Facile synthesis of silver nanoparticles stabilized by cationic polynorbornenes and their catalytic activity in 4-nitrophenol reduction *Langmuir* **29** 4225–4234
10. Hemmaragala N M, Abrahamse H, George B P A, Gannimani R and Govender P 2016 Functionalized silver nanoparticle catalyzed [3+2] rycloaddition reaction: Greener route to substituted-1,2,3-triazolines *Catal. Letters* **146** 464–473
11. Kim A Y, Bae H S, Park S, Park S and Park K H 2011 Silver nanoparticle catalyzed selective hydration of nitriles to amides in water under neutral conditions *Catal. Lett.* **141** 685–690
12. Fišera R, Králik M, Annus J, Krátky V, Zecca M and Hronec M 1997 Deactivation of polymer-supported palladium catalysts in the hydrogenation of 4-nitrotoluene *Collect. Czechoslov. Chem. Commun.* **62** 1763–1775
13. Centomo P, Zecca M, Lora S, Vitulli G, Caporusso A, Tropeano M, Milone C, Galvagno S and Corain B 2005 Novel Pt catalysts supported on functional resins for the chemoselective hydrogenation of citral to the-unsaturated alcohols geraniol and nerol *J. Catal.* **229** 283–297

14. Michalska Z M and Strzelec K 2001 Rhodium(I) complex catalysts immobilized on polyamides having a pyridine moiety: Effect of the polymer structure *J. Mol. Catal. A Chem.* **177** 89–104
15. Biffis A, Corain B, Cvengrosova Z, Hronec M, Jerabek K and Kralik M 1995 Relationships between physicochemical properties and catalytic activity of polymer-supported Part I . Experimental investigations *Appl. Catal. A Gen.* **124** 355–365
16. Zharmagambetova A K, Golodov V A and Saltykov Y P 1989 The study of the composition and catalytic properties of palladium(II) complexes with poly(vinylpyridine) *J. Mol. Catal.* **55** 406–414
17. Zharmagambetova A K, Ergozhin E E, Sheludyakov Y L, Mukhamedzhanova S G, Kurmanbayeva I A, Selenova B A and Utkelov B A 2001 2-Propen-1-ol hydrogenation and isomerisation on polymer-palladium complexes-effect of polymer matrix *J. Mol. Catal. A Chem.* **177** 165–170
18. Pomogailo A D and Kestelman V N 2005 *Metallopolymer nanocomposites* (Berlin Heidelberg New York: Springer Series in materials science)
19. Hodge P 1997 Polymer-supported organic reactions: What takes place in the beads? *Chem. Soc. Rev.* **26** 417–424
20. Corain B, Zecca M and Jeřábek K 2001 Catalysis and polymer networks - The role of morphology and molecular accessibility *J. Mol. Catal. A Chem.* **177** 3–20
21. Fu L P, Shi Q Q, Shi Y, Jiang B and Tu S J 2013 Three-component domino reactions for regioselective formation of bis-indole derivatives *ACS Comb. Sci.* **15** 135–140
22. Zhang R, Zhang D, Guo Y, Zhou G, Jiang Z and Dong D 2008 Vilsmeier reaction of enaminones: Efficient synthesis of halogenated pyridin-2(1H)-ones *J. Org. Chem.* **2** 9504–9507
23. Abass M and Mostafa B B 2005 Synthesis and evaluation of molluscicidal and larvicidal activities of some novel enaminones derived from 4-hydroxyquinolinones: Part IX *Bioorganic Med. Chem.* **13** 6133–6144
24. Sun J, Dong Z, Li P, Zhang F, Wei S, Shi Z and Li R 2013 Ag nanoparticles in hollow magnetic mesoporous spheres: A highly efficient and magnetically separable catalyst for synthesis of β-enaminones *Mater. Chem. Phys.* **140** 1–6
25. Eddington N D, Cox D S, Khurana M, Salama N N, Stables J P, Harrison S J, Negussie A, Taylor R S, Tran U Q, Moore J A, Barrow J C and Scott K R 2003 Synthesis and anticonvulsant activity of enaminones - Part 7. Synthesis and anticonvulsant evaluation of ethyl 4-[(substituted phenyl)amino]-6-methyl-2-oxocyclohex-3-ene-1-carboxylates and their corresponding 5-methyl-cyclohex-2-enone derivatives *Eur. J. Med. Chem.* **38** 49–64
26. Zhang Z H, Li T S and Li J J 2007 Synthesis of enaminones and enamino esters catalysed by $ZrOCl_2.8H_2O$ *Catal. Commun.* **8** 1615–1620
27. Brandt C A, Da Silva A C M P, Pancote C G, Brito C L and Da Silveira M A B 2004 Efficient synthetic method for β-enamino esters using ultrasound *Synthesis (Stuttg).* 1557–1559
28. Rechsteiner B, Texier-Boullet F and Hamelin J 1993 Synthesis in dry media coupled with microwave irradiation: Application to the preparation of enaminoketones. *Tetrahedron Lett.* **34** 5071–5074
29. Bartoli G, Bosco M, Locatelli M, Marcantoni E, Melchiorre P and Sambri L 2004 $Zn(ClO_4)_2{\cdot}6H_2O$ as a powerful catalyst for the conversion of β-ketoesters into β-enamino esters *Synlett* 0239–0242
30. Zhang Z H, Yin L and Wang Y M 2006 A general and efficient method for the preparation of β-enamino ketones and esters catalyzed by indium tribromide *Adv. Synth. Catal.* **348** 184–190
31. Epifano F, Genovese S and Curini M 2007 Ytterbium triflate catalyzed synthesis of β-enaminones *Tetrahedron Lett.* **48** 2717–2720
32. Zhang Z H and Hu J Y 2006 Cobalt(II) chloride-mediated synthesis of β-enamino compounds under solvent-free conditions *J. Braz. Chem. Soc.* **17** 1447–1451
33. Das B, Venkateswarlu K, Majhi A, Reddy M R, Reddy K N, Rao Y K, Ravikumar K and Sridhar B 2006 Highly efficient, mild and chemo- and stereoselective synthesis of enaminones and enamino esters using silica supported perchloric acid under solvent-free conditions *J. Mol. Catal. A Chem.* **246** 276–281
34. Siddiqui Z N, Khan K and Ahmed N 2014 Nano fibrous silica sulphuric acid as an efficient catalyst for the synthesis of β-enaminone *Catal. Letters* **144** 623–632
35. Hariprasad E and Radhakrishnan T P 2010 A highly efficient and extensively reusable "dip catalyst" based on a silver-nanoparticle-embedded polymer thin film *Chem. - A Eur. J.* **16** 14378–14384
36. Chtchigrovsky M, Lin Y, Ouchaou K, Chaumontet M, Robitzer M, Quignard F and Taran F 2012 Dramatic effect of the gelling cation on the catalytic performances of alginate-supported palladium nanoparticles for the Suzuki-Miyaura reaction *Chem. Mater.* **24** 1505–1510
37. Wilson M, Kore R, Fraser R C, Beaumont S K, Srivastava R and Badyal J P S 2017 Recyclable palladium catalyst cloths for carbon-carbon coupling reactions *Colloids Surfaces A Physicochem. Eng. Asp.* **520** 788–795
38. Xia M, Kang S M, Lee G W, Huh Y S and Park B J 2019 The recyclability of alginate hydrogel particles used as a palladium catalyst support *J. Ind. Eng. Chem.* **73** 306–315
39. Wang Z, Zhang H, Li L, Miao S, Wu S, Hao X, Zhang W and Jia M 2018 Polyacrylonitrile beads supported Pd-based nanoparticles as superior catalysts for dehydrogenation of formic acid and reduction of organic dyes *Catal. Commun.* **114** 51–55
40. Gholap A R, Chakor N S, Daniel T, Lahoti R J and Srinivasan K V. 2006 A remarkably rapid regioselective synthesis of β-enaminones using silica chloride in a heterogeneous as well as an ionic liquid in a homogeneous medium at room temperature *J. Mol. Catal. A Chem.* **245** 37–46
41. Carotenuto G, Pepe G P and Nicolais L 2000 Preparation and characterization of nano-sized Ag/PVP composites for optical applications *Eur. Phys. J. B* **16** 11–17
42. Porel S, Singh S, Harsha S S, Rao D N and Radhakrishnan T P 2005 Nanoparticle-embedded polymer: In situ synthesis, free-standing films with highly monodisperse silver nanoparticles and optical limiting *Chem. Mater.* **17** 9–12

43. Prasad B L V, Stoeva S I, Sorensen C M and Klabunde K J 2003 Digestive-ripening agents for gold nanoparticles: Alternatives to thiols *Chem. Mater.* **15** 935–942
44. Zhang S, Zhang L, Liu K, Liu M, Yin Y and Gao C 2018 Digestive ripening in the formation of monodisperse silver nanospheres *Mater. Chem. Front.* **2** 1328–1333
45. Koczkur K M, Mourdikoudis S, Polavarapu L and Skrabalak S E 2015 Polyvinylpyrrolidone (PVP) in nanoparticle synthesis *Dalt. Trans.* **44** 17883–17905
46. Si R, Zhang Y W, You L P and Yan C H 2006 Self-organized monolayer of nanosized ceria colloids stabilized by poly(vinylpyrrolidone) *J. Phys. Chem. B* **110** 5994–6000
47. Saha B, Kumar S and Sengupta S 2019 Green synthesis of nano silver on TiO_2 catalyst for application in oxidation of thiophene *Chem. Eng. Sci.* **199** 332–341
48. Isaifan R J, Ntais S and Baranova E A 2013 Particle size effect on catalytic activity of carbon-supported Pt nanoparticles for complete ethylene oxidation *Appl. Catal. A Gen.* **464–465** 87–94
49. Ahmed N and Siddiqui Z N 2014 Mesoporous alumina sulphuric acid: A novel and efficient catalyst for on-water synthesis of functionalized 1,4-dihydropyridine derivatives via β-enaminones *J. Mol. Catal. A Chem.* **394** 232–243
50. Park S, Park S, An J, An J, Jung I, Jung I, Piner R D, Piner R D, An S J, An S J, Li X, Li X, Velamakanni A, Velamakanni A, Ruoff R S and Ruoff R S 2009 Colloidal suspensions of highly reduced graphene oxide in a wide variety of organic solvents. *Nano Lett.* **9** 1593–1597